Simulations of Water-Air Flows with Low and High Pressure Ratios

Dr. Shaban Jolgam [1], Dr. Ahmed Ballil[2], and Dr Andrew Nowakowski[3]
[1]Dept. of Mechanical engineering, Zawia University
[2]Dept. of Mechanical engineering, Benghazi University,
[3]Dept. of Mechanical engineering, Sheffield University, Sheffield, UK

Abstract:

Numerical simulation of two phase flows, which includes interface creation and evolution, is a challenging task due to its complexity. In this contribution, simulations of water-air flows characterised by high and low pressure jumps across the interface are presented. A computer program using "C" language is developed to compute a fully non-equilibrium two-phase flow model. The model consists of seven partial differential equations in one dimensional flow as follows: mass, momentum and energy equations for each constituent augmented by a volume fraction evolution

equation for one of the constituents. A diffuse interface numerical method is employed to capture the interface evolution in different water-air flow regimes. This method is based on an extended second order finite volume Godunov-type approach. A fixed Eulerian mesh is built and fluxes at each cell boundaries are computed using an efficient HLL approximate Riemann solver. Velocity and pressure relaxation procedures are applied to fulfill the interface conditions. Two case studies are considered to verify the developed code. The first case considers the water-air shock tube problem, which provides a high pressure ratio of (10^4) and the second test considers the water-faucet flow, which provides a low pressure ratio of (1). The obtained results show very good agreement with both the exact solutions and other published results.

***Keywords**: compressible multiphase flow, hyperbolic PDEs, Riemann problem, Godunov methods, shock waves, HLL Riemann solver.*

1. Introduction:

Numerical modeling of multiphase flows has been developed enormously in recent years. In this context, many mathematical models have been derived and many numerical approaches have been developed and applied to represent the complex physics of multiphase flows. This paper is concerned with the numerical simulation of multiphase flows, in particular water-air flows. These flows are common in many natural phenomena, hydraulic engineering and industrial applications. For example, rain, bubbly flows, cavitations' phenomenon, water jet flows, thermal and chemical plants.

Many investigations were conducted to study the physical behavior of different air-water flow regimes. For instance, the air-water flow field

which includes air bubble sizes, air bubble distributions, air-water velocity profiles and bubble-turbulence interactions was studied and analyzed in the theme of air entrainment processes in free-surface turbulent flows in [1]. The two phase air-water flows in vertical capillary tubes were studied and some flow characteristics such as void fraction, frictional pressure loss and rise velocity of slug bubbles were measured in [2]. Numerical simulations of multiphase air-water flows through high pressure nozzles were presented in [3]. Recently, Air-water interactions in hydraulic jump were simulated using a mesh-free particle (Lagrangian) method in [4].

Numerically, there are two main approaches that are widely used to simulate multiphase flows including air-water flows. These are: Sharp Interface Methods (SIM) and Diffuse Interface Methods (DIM). The SIM methods consider interfaces between flow constituents as sharp non-smeared discontinuities. consequently, the approaches under this category eliminating numerical diffusion at the interfaces completely, which means the artificial mixing problem is eliminated as well. This is the main advantage of the SIM over the DIM, however, other numerical and practical difficulties may possibly occur. Some well-known examples of these methods are the interface tracking methods [5], arbitrary Lagrangian-Eulerian methods [6], volume of fluid methods [7,8] and level set methods[9].

On the other hand, the DIM methods allow numerical diffusion at the interface. Although numerical diffusion is considered as a weakness for numerical methods, it is an essential feature for capturing any flow discontinuities. There are a number of ways to reduce the effect of numerical diffusion at the interface. For example, mesh refinement and using high order numerical schemes. Nevertheless, these methods are

relatively easier and more flexible in coding and implementation than SIM. The DIM mainly divided into two groups of methods: the first group is based on Euler equations as presented for example in [10,11]. These methods are easy to implement and very efficient for simulating flows with relatively simple physical problems. However, they suffer the lake of accuracy in computing internal energies and temperatures at interfaces. The second group is based on multiphase flow equations. These models are more suitable for solving multiphase flow problems than the Euler equations. They are able to deal with general equations of state, conservative for mixtures and provide precise internal energies and temperatures at interfaces. Good examples of these models are the *parent model* developed in [12], the transport multiphase model proposed in [13], the reduced multiphase model derived in [14] and the six equation model developed in [15,16].

In this work the hyperbolic, non-equilibrium, multiphase flow model that presented in [17] is adopted to simulate different air-water flow regimes. A numerical framework based on Godunov type approach is implemented within a newly developed "C" language code. Both velocity and pressure relaxation terms are taken into account during the computations. The main challenge is to simulate the water-air flows with low and high pressure jumps across the interface.

This paper is organized as follows: The mathematical formulation of the governing equations of the two-phase flow models are reviewed in the next section. Then the numerical method is described with the HLL Riemann solver. After that, the case studies and obtained results are presented. Finally, the conclusions are derived.

2. Mathematical formulation:

For most two-phase flow problems with interfaces that move and deform, the local instant formulation based on the single-phase equations encounters mathematical and numerical difficulties. Hence, a suitable averaging method has become essential to continuously eliminate interfacial discontinuities and make a two-phase flow as a continuum formulation [18].

A compressible two-phase flow model can be obtained by applying the averaging method of Drew presented in [19] to the Navier-Stokes equations for single-phase flow. Saurel and Abgrall in [12] have developed a multiphase flow model by applying this method and considering all dissipative terms at the interfaces and neglecting them everywhere else. Their model, which is known later as the *parent* model, was inspired by the work of Baer and Nunziato which was presented in [20]. The model of Baer and Nunziato was proposed to study the deflagration-to-detonation transition in solid energetic materials. The model of [12] is similar to that of [20] but they have introduced different treatments of the interfacial variables and relaxation parameters. These treatments have extended the range of applications of the parent model which can be written in one dimension without heat and mass transfer terms in the following form:

$$\frac{\partial \alpha_1}{\partial t} + u_{\text{int}} \frac{\partial \alpha_1}{\partial x} = \mu(p_1 - p_2) \qquad (1a)$$

$$\frac{\partial \alpha_1 \rho_1}{\partial t} + \frac{\partial \alpha_1 \rho_1 u_1}{\partial x} = 0 \qquad (1b)$$

$$\frac{\partial \alpha_1 \rho_1 u_1}{\partial t} + \frac{\partial \left(\alpha_1 \rho_1 u_1^2 + \alpha_1 p_1\right)}{\partial x} = p_{\text{int}} \frac{\partial \alpha_1}{\partial x} + \lambda(u_2 - u_1) + \alpha_1 \rho_1 g \qquad (1c)$$

$$\frac{\partial \alpha_1 \rho_1 E_1}{\partial t} + \frac{\partial u_1 (\alpha_1 \rho_1 E_1 + \alpha_1 p_1)}{\partial x} = p_{\text{int}} u_{\text{int}} \frac{\partial \alpha_1}{\partial x} + \lambda u_{\text{int}} (u_2 - u_1) + \mu p_{\text{int}} (p_1 - p_2) + \alpha_1 \rho_1 u_1 g \quad (1d)$$

$$\frac{\partial \alpha_2 \rho_2}{\partial t} + \frac{\partial \alpha_2 \rho_2 u_2}{\partial x} = 0 \quad (1e)$$

$$\frac{\partial \alpha_2 \rho_2 u_2}{\partial t} + \frac{\partial (\alpha_2 \rho_2 u_2^2 + \alpha_2 p_2)}{\partial x} = -p_{\text{int}} \frac{\partial \alpha_1}{\partial x} - \lambda (u_2 - u_1) + \alpha_2 \rho_2 g \quad (1f)$$

$$\frac{\partial \alpha_2 \rho_2 E_2}{\partial t} + \frac{\partial u_2 (\alpha_2 \rho_2 E_2 + \alpha_2 p_2)}{\partial x} = -p_{\text{int}} u_{\text{int}} \frac{\partial \alpha_1}{\partial x} - \lambda u_{\text{int}} (u_2 - u_1) - \mu p_{\text{int}} (p_1 - p_2) + \alpha_2 \rho_2 u_2 g \quad (1g)$$

where $\alpha_k, \rho_k, u_k, p_k$ and E_k are the volume fraction, the density, the velocity, the pressure and the total energy for the phase k (1, 2), respectively; p_{int} and u_{int} are the interfacial pressure and velocity, respectively; g is the gravitational force; $E_k = e_k + \frac{1}{2} u_k^2$ where e_k is the specific internal energy of the phase k.

The non-conservative coupling terms $p_{\text{int}} \frac{\partial \alpha_k}{\partial x}$ and $p_{\text{int}} u_{\text{int}} \frac{\partial \alpha_k}{\partial x}$ which appear on the right hand side of the momentum (1c, 1f) and energy (1d, 1g) equations are resulted from the averaging process. These terms cannot be written in the divergence form, i.e. conservative form. Hence, the model is a non-conservative model. To circumvent the non-conservative character of this model, the Abgrall's idea proposed in [21] is considered

The terms on the right hand side of the momentum and energy equations that contain gravitational force are considered only when the

gravity has a significant effect such as in the water- faucet test, which is conducted in this work.

2.1 Closure relations:

Extra terms, which represent the transfer processes that may take place at the interface, appear in the model result from the averaging process used to derive the model (1). These terms are unknown. Volume fractions, which are known and indicate the presence of each phase within the computational cell, for each phase also appear on the right hand side of the model (1). Originally the multiphase flow model (1) consists of two mass equations (1b, 1e), two momentum equations (1c, 1f) and two energy equations (1d, 1g). The number of these equations is six which is less than the number of the unknown variables which are twelve. Therefore, the following relations are considered to close the model (1):

Evolution equation for volume fraction (1a) is added to the model (1) as proposed by [22].

Volume fraction constraint which may be written as follows:

$$\alpha_1 + \alpha_2 = 1 \qquad (2)$$

Equations of state are used to link the thermodynamic variables within each phase. In this work stiffened equation of state is considered to govern the working fluids. The stiffened equation of state may be written in the following form:

$$p = (\gamma - 1)\rho e - \gamma \pi \qquad (3)$$

where γ is the adiabatic specific heat ratio and π is the pressure constant they depend on the material under consideration.

The interfacial pressure is assumed to be equal to the mixture pressure [12]:

$$p_{\text{int}} = \sum_k p_k \alpha_k \qquad (4)$$

The interfacial velocity is assumed to be equal to the mixture velocity [12]:

$$u_{\text{int}} = \frac{\sum_k \alpha_k \rho_k u_k}{\sum_k \alpha_k \rho_k} \qquad (5)$$

2.2 Pressure relaxation terms:

The pressure relaxation term $\mu(p_1 - p_2)$ which appears on the right hand side of the volume fraction evolution equation (1a) expresses the expansion rate of the volume fraction. The expansion rate drives the pressure to equilibrium. The other pressure relaxation term $\mu p_{\text{int}}(p_1 - p_2)$ which appears on the right hand side of the energy equations (1d, 1g) expresses the pressure work done by the phases to achieve the pressure equilibrium. The variable μ controls the rate at which the pressure relaxation process takes place; its value grows to be infinite at the interface in order the process takes place in a short time [17].

2.3 Velocity relaxation terms:

The velocity relaxation terms $\lambda(u_2 - u_1)$ and $\lambda u_{\text{int}}(u_2 - u_1)$ which appear on the right hand side of the momentum equations (1c, 1f) and energy equations (1d, 1g), respectively, are responsible for driving both phases to relax to a common velocity at the interface. The value of the variable λ has to be infinite increase the rate at which the velocity relaxation process takes place rapidly [17].

3. Numerical method:

The exact analytical solution of the multiphase flow model (1) is unknown [23]. Therefore, the only choice is to solve it numerically. However, the numerical solution of this model is not easy due to the presence of the non-conservative equation of the evolution of volume fraction (1a), the non-conservative terms existing on the right hand side of the momentum equations (1c, 1f) and energy equations (1d, 1g) and the relaxation term that appear on the right hand side of the model as mentioned earlier. Therefore, numerical solution can be attained by splitting the model into hyperbolic part operator $L_h^{\Delta t}$ and source and relaxation part operator $L_s^{\Delta t}$ and solving them using the Strang splitting technique which may be written in second order as follows:

$$U_i^{n+1} = L_s^{\Delta t/2} L_h^{\Delta t} L_s^{\Delta t/2} U_i^n \tag{6}$$

where U_i^{n+1} and U_i^n are the vectors of conservative variables at times $n+1$ and n, respectively. The hyperbolic part and source and relaxation part operators have to be solved in succession as given in [17].

3.1 The hyperbolic operator:

The hyperbolic part of the two-phase flow model (1) can be written as follows:

$$\frac{\partial \alpha_1}{\partial t} + u_{\text{int}} \frac{\partial \alpha_1}{\partial x} = 0 \tag{7a}$$

$$\frac{\partial U}{\partial t} + \frac{\partial F(U)}{\partial x} = H(U) \frac{\partial \alpha_1}{\partial x} \tag{7b}$$

where U, $F(U)$ and $H(U)$ are the vectors of conserved variables, fluxes and non-conservative, they are given respectively as follows:

$$U=\begin{bmatrix}\alpha_1\rho_1\\ \alpha_1\rho_1u_1\\ \alpha_1\rho_1E_1\\ \alpha_2\rho_2\\ \alpha_2\rho_2u_2\\ \alpha_2\rho_2E_2\end{bmatrix},\quad F(U)=\begin{bmatrix}\alpha_1\rho_1u_1\\ \alpha_1\rho_1u_1^2+\alpha_1p_1\\ u_1(\alpha_1\rho_1E_1+\alpha_1p_1)\\ \alpha_2\rho_2u_2\\ \alpha_2\rho_2u_2^2+\alpha_2p_2\\ u_2(\alpha_2\rho_2E_2+\alpha_2p_2)\end{bmatrix}\text{ and }H(U)=\begin{bmatrix}0\\ p_i\\ p_{\text{int}}u_{\text{int}}\\ 0\\ -p_{\text{int}}\\ -p_{\text{int}}u_i\end{bmatrix}.$$

The solution of the hyperbolic system (7) is not direct as for the Euler equations due to the existence of the non-conservative equation (7a) of the volume fraction. The solution can be attained by applying the Godunov-type scheme which is used to discretise the non-conservative system (7). To obtain a second order accuracy in time and space the MUSCL scheme is applied [24]. The discretisation of the system (7) can be written as follows:

$$\alpha_i^{n+1}=\alpha_i^n-\frac{\Delta t}{\Delta x}u_i\left[\alpha^*(\alpha_{i+1/2}^-,\alpha_{i+1/2}^+)-\alpha^*(\alpha_{i-1/2}^-,\alpha_{i-1/2}^+)\right] \qquad (8a)$$

$$U_i^{n+1}=U_i^n-\frac{\Delta t}{\Delta x}\Big[F(U^*(U_{i+1/2}^-,U_{i+1/2}^+))-F(U^*(U_{i-1/2}^-,U_{i-1/2}^+))\Big]+\Delta t\,H(U_i^{n+1/2})\Delta_i \qquad (8b)$$

where F is the numerical flux vector calculated at the intercell boundaries $x_{i\pm1/2}$ between $U_{i-1/2}^+$ and $U_{i+1/2}^+$, Δ_i is the discretization of the volume fraction $\frac{\partial\alpha_1}{\partial x}$ in space which depends on the approximate Riemann

solver [17] and $H(U_i^{n+1/2})$ is the vector of non-conservative terms. The time step is computed using the following expression:

$$\Delta t = \frac{\text{CFL}\,\Delta x}{S_{\text{Max}}} \tag{9}$$

where CFL is the Courant number; for stability it has to be less than one, Δx is the cell size and S_{Max} is the maximum wave speed. The left and right wave speeds at the boundaries $S^-_{i\pm1/2}$ and $S^+_{i\pm1/2}$ can be computed for the two phases respectively by:

$$S^-_{i\pm1/2} = \min(u^+_{k,i\pm1/2} - c^+_{k,i\pm1/2}, u^-_{k,i\pm1/2} - c^-_{k,i\pm1/2}), \tag{10a}$$

$$S^+_{i\pm1/2} = \max(c^+_{k,i\pm1/2} + u^+_{k,i\pm1/2}, c^-_{k,i\pm1/2} + u^-_{k,i\pm1/2}), \tag{10b}$$

where *k* represents the phases 1 and 2.

3.2 The HLL approximate Riemann solver:

This approximate Riemann solver which is presented in [25] is based on a minimum S^- and maximum S^+ wave speeds arising in the Riemann solution. The solver uses a single intermediate state (*) enclosed between these two waves. According to this solver the fluxes may be computed using the following expression:

$$F^{hll}_{1\pm\frac{1}{2}} = \begin{cases} F_L & \text{if } S^-_{i\pm1/2} \geq 0, \\ F^{hll} & \text{if } S^+_{i\pm1/2} \geq 0 \geq S^-_{i\pm1/2}, \\ F_R & \text{if } S^+_{i\pm1/2} \leq 0. \end{cases} \tag{11a}$$

$$F^{hll}_{i\pm1/2} = \frac{S^+_{i\pm1/2}F_L - S^-_{i\pm1/2}F_R + S^-_{i\pm1/2}S^+_{i\pm1/2}(U_R - U_L)}{S^+_{i\pm1/2} - S^-_{i\pm1/2}}. \tag{11b}$$

According to the HLL solver the discretization of the volume fraction equation (8a) in space and time may be rewritten as follows:

$$\alpha_i^{n+1} = \alpha_i^n - \frac{\Delta t}{\Delta x}\left[\frac{u_i^{n+1/2}(S_{i+1/2}^{+}\alpha_{i+1/2,-}^{n+1/2} - S_{i+1/2}^{-}\alpha_{i+1/2,+}^{n+1/2})}{S_{i+1/2}^{+} - S_{i+1/2}^{-}} + \frac{S_{i+1/2}^{+}S_{i+1/2}^{-}(\alpha_{i+1/2,+}^{n+1/2} - \alpha_{i+1/2,-}^{n+1/2})}{S_{i+1/2}^{+} - S_{i+1/2}^{-}} - \right.$$

$$\left.\frac{u_i^{n+1/2}(S_{i-1/2}^{+}\alpha_{i-1/2,-}^{n+1/2} - S_{i-1/2}^{-}\alpha_{i-1/2,+}^{n+1/2})}{S_{i-1/2}^{+} - S_{i-1/2}^{-}} - \frac{S_{i-1/2}^{+}S_{i-1/2}^{-}(\alpha_{i-1/2,+}^{n+1/2} - \alpha_{i-1/2,-}^{n+1/2})}{S_{i-1/2}^{+} - S_{i-1/2}^{-}}\right] \quad (12)$$

and the discretization of the volume fraction in space Δ_i in the equation (8b) according to the HLL solver may be written as follows:

$$\Delta_i = \frac{1}{\Delta x}\left[\frac{S_{1+1/2}^{+}\alpha_{i+1/2,-}^{n+1/2} - S_{1+1/2}^{-}\alpha_{i+1/2,+}^{n+1/2}}{S_{1+1/2}^{+} - S_{1+1/2}^{-}} - \frac{S_{1-1/2}^{+}\alpha_{i-1/2,-}^{n+1/2} - S_{1-1/2}^{-}\alpha_{i-1/2,+}^{n+1/2}}{S_{1-1/2}^{+} - S_{1-1/2}^{-}}\right] \quad (13)$$

3.3 The relaxation and source terms operator :

The relaxation and source terms operator part of the two-phase flow model (1) is an ordinary differential equations ODE which can be written as follows:

$$\frac{dQ}{dt} = D_V + D_P + D_S\,, \quad (14)$$

where Q, D_V, D_P, D_S represent the volume fraction and the conserved variables, the velocity relaxation parameters, the pressure relaxation parameters and the source terms, respectively, They are defined as follows:

$$Q = \begin{bmatrix} \alpha_1 \\ \alpha_1\rho_1 \\ \alpha_1\rho_1 u_1 \\ \alpha_1\rho_1 E_1 \\ \alpha_2\rho_2 \\ \alpha_2\rho_2 u_2 \\ \alpha_2\rho_2 E_2 \end{bmatrix},\ D_V = \begin{bmatrix} 0 \\ 0 \\ \lambda(u_2 - u_1) \\ u_{\text{int}}\lambda(u_2 - u_1) \\ 0 \\ -\lambda(u_2 - u_1) \\ -u_{\text{int}}\lambda(u_2 - u_1) \end{bmatrix}, D_P = \begin{bmatrix} \mu(p_1 - p_2) \\ 0 \\ 0 \\ p_{\text{int}}\mu(p_1 - p_2) \\ 0 \\ 0 \\ -p_{\text{int}}\mu(p_1 - p_2) \end{bmatrix} \text{ and } D_S = \begin{bmatrix} 0 \\ 0 \\ \alpha_1\rho_1 g \\ \alpha_1\rho_1 u_1 g \\ 0 \\ \alpha_2\rho_2 g \\ \alpha_2\rho_2 u_2 g \end{bmatrix}. \quad (15)$$

The solution of the ODE (14) is obtained by solving the integration operators using the Strang method:

$$Q_i^{n+1} = L_V^{\Delta t} L_P^{\Delta t} L_s^{\Delta t} Q_i^n \qquad (16)$$

where the operators L_V, L_P, L_S are defined by the vectors D_V, D_P, D_S, respectively, given by (15). Internal energy for both phases must be updated after velocity relaxation process. Velocity and pressure relaxation processes have to be done every time step. The effect of gravity is considered by solving the source term operator when it has a significant effect.

4. Test problems and results:

The assessment of the performance of the developed algorithm was carried out using carefully chosen test problems. These test problems represent two different test cases where the pressure ratio between the two flow constituents varies from a very high pressure ratio of (10^4) to a very low pressure ratio of (1). A necessary assumption is usually made for numerical simulations of two-phase flows using diffuse interface methods. The assumption is that a presence of a negligible volume fraction $\varepsilon = 10^{-8}$ of the second phase in the first phase which is considered as a pure phase.

4.1 Water-air shock tube:

This is a standard water-air shock tube test problem used to assess the ability of the developed code to simulate problems with flow constituents that have very high pressure ratios. The tube is 1 m long and divided to two chambers. The left hand chamber is filled with water at a higher pressure and the right hand chamber is filled with air at atmospheric pressure. The interface which separates the two fluids is located at $x = 0.7$

m. Both fluids are governed by the stiffened gas equation of state. The stiffened gas equation of state parameters for air are $\gamma = 1.4$, $\pi = 0\,\text{Pa}$ and for water are $\gamma = 4.4$, $\pi = 6\times10^{8}\,\text{Pa}$. The initial conditions for both components are:

$$(\rho, u, p) = \begin{cases} 1000, 0, 10^{9} & \text{if } x < 0.7, \\ 50, 0, 10^{5} & \text{if } x > 0.7. \end{cases} \qquad (17)$$

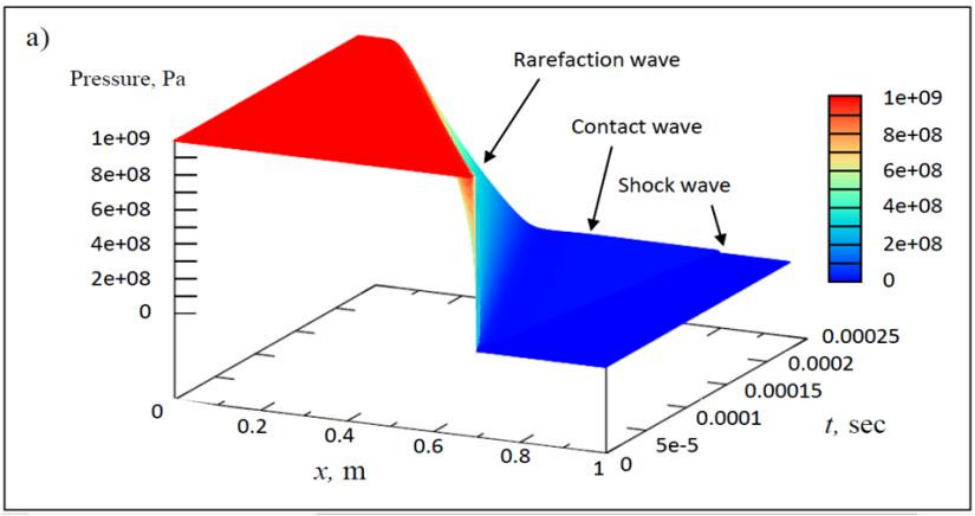

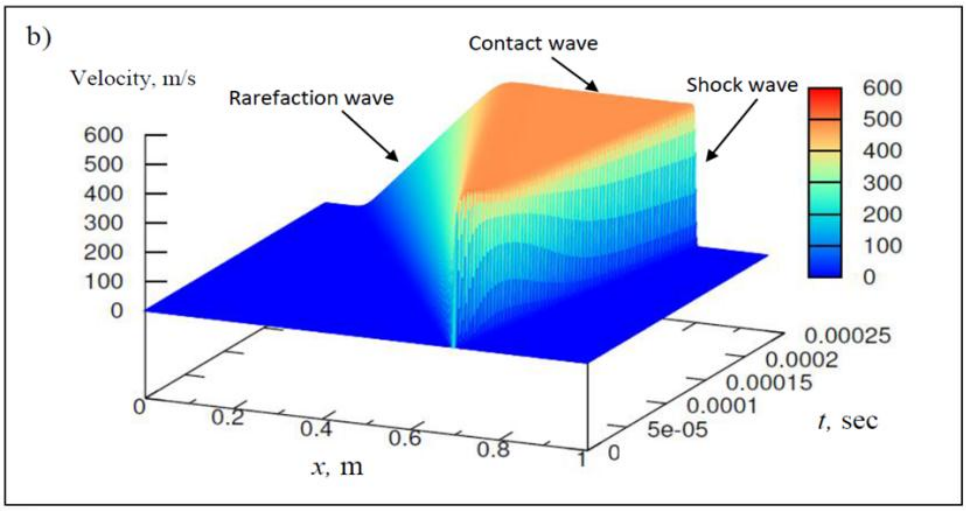

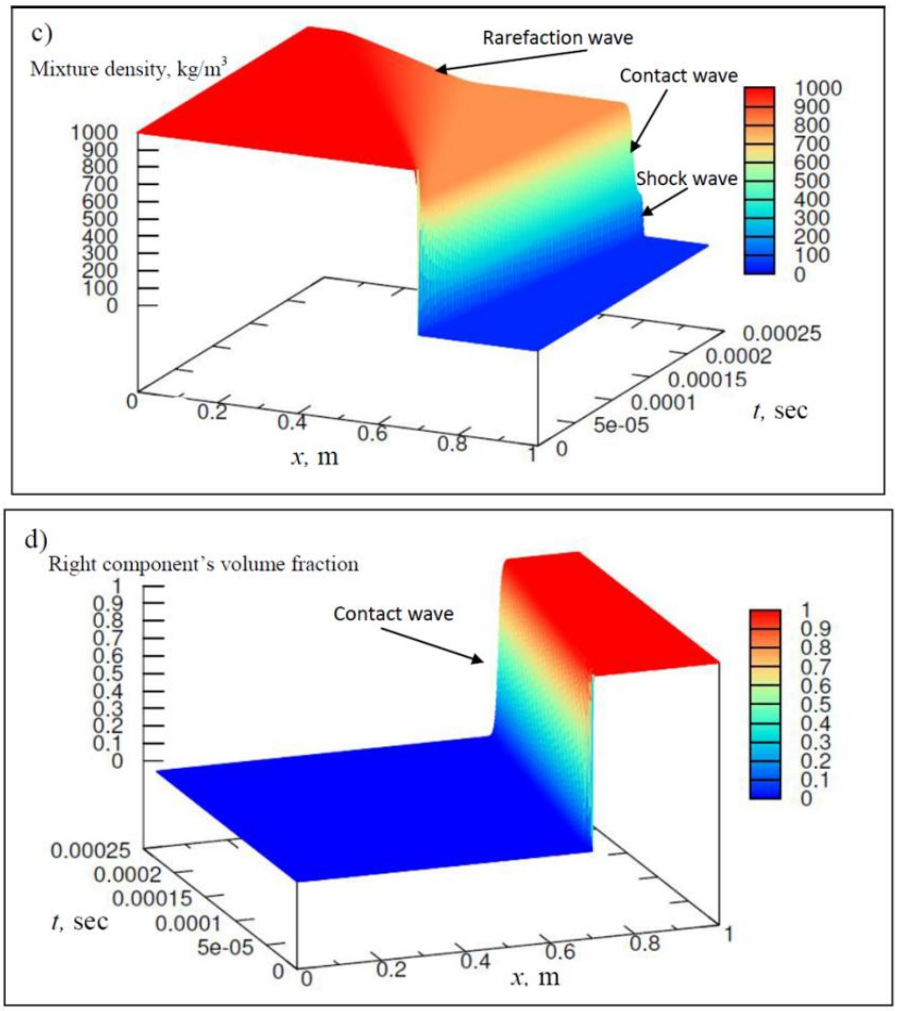

Figure 1. Water-air test: Surface plot for time evolution for: (a) pressure, (b) velocity, (c) mixture density and (d) volume fraction.

Initially both constituents are at rest, as soon as the membrane separating the two components is removed, the water which has the higher pressure and density starts to move to the right. Therefore, strong shock and contact discontinuity waves are generated which move to the right and a rarefaction wave is generated which moves to the left. The numerical

results are obtained from the HLL approximate Riemann solver using 200 cells with the CFL = 0.9. The surface and contour plots for the results of time evolution for pressure (a), velocity (b), mixture density (c) and volume fraction (d) are show in Figure 1 and Figure 2, respectively. One can notice clearly the shock and rarefaction waves from the velocity contour plot (b) in Figure 2.

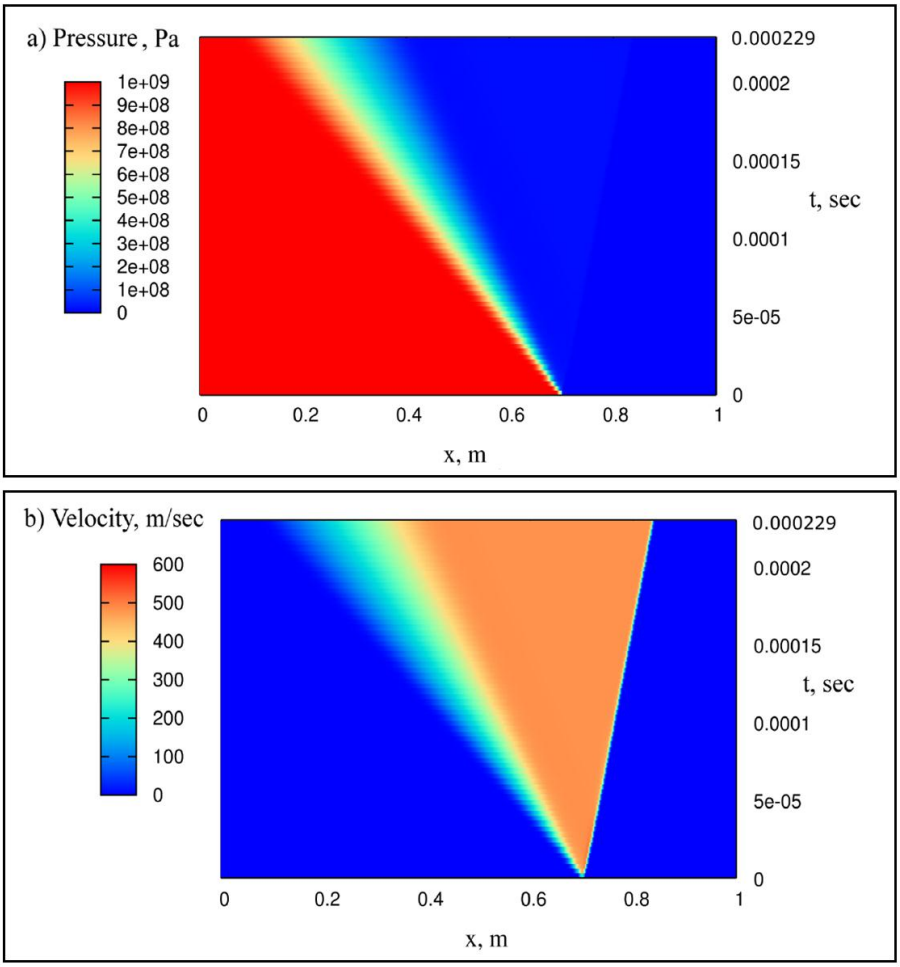

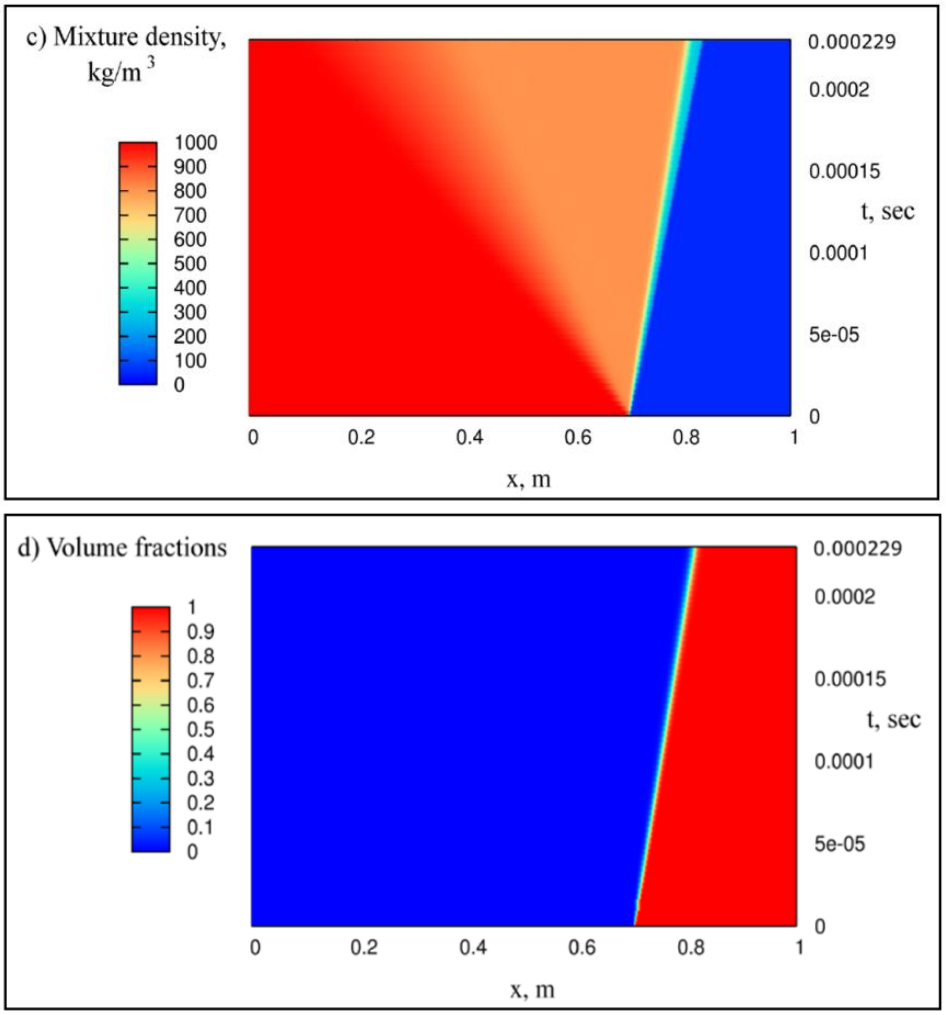

Figure 2. Water-air test: Contour plot for time evolution for: (a) pressure, (b) velocity, (c) mixture density and (d) volume fraction.

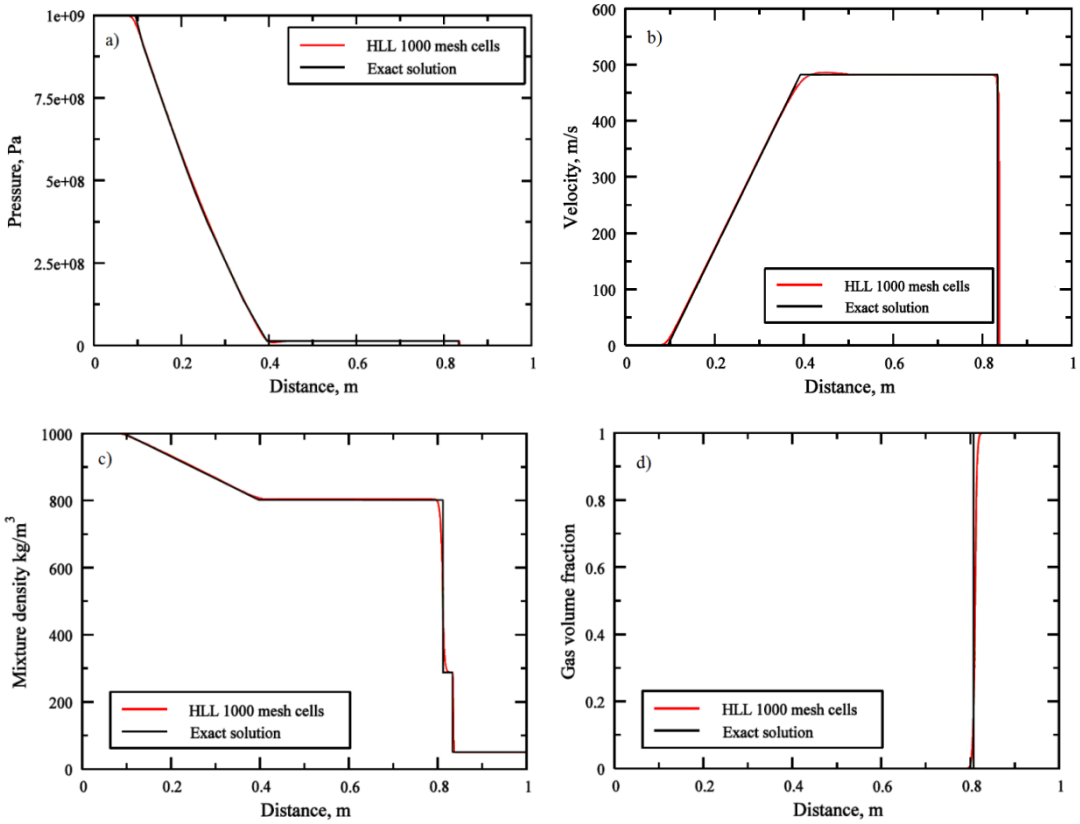

Figure 3. Water-air test: results of (a) pressure, (b) velocity, (c) mixture density and (d) volume fraction at t = 229 μs.

The results of pressure (a), velocity (b), mixture density (c) and volume fraction (d) for this test are obtained using 1000 cells and compared to the exact solution at t = 229 μs as shown in Figure 3. It can be observed that the results are in a good agreement with the exact solution.

4.2 Water-faucet test:

This test was proposed by Ransom in [26] to study behavior of incompressible two-phase flows. The test is chosen to be simulated using the model (1) which was basically proposed for compressible two-phase

flows. The test consists of a vertical tube with open ends. The tube depth is 12 m and contains of a water column which is surrounded by air. The water leaves the faucet and enters the tube at atmospheric pressure with velocity of $10\,\mathrm{m/s}$ and volume fraction of 0.8. Several stages are presented in Figure 4. Under the effect of gravity, the water accelerates and narrows as it passes through the tube to maintain mass conservation. Therefore, the gravitational effect is considered in the calculations for this test. At the interface, which separates the flow components, each component has different direction and hence the velocity relaxation is not performed in the numerical solution of this test.

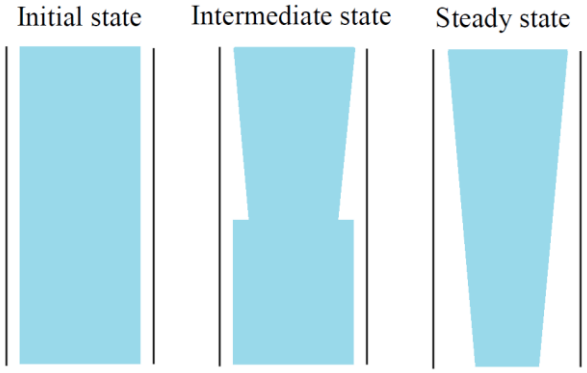

Figure 4. Water-faucet test.

The initial conditions are as follows:

$$(\rho, u, p, \alpha) = \begin{cases} 1000, 10, 10^5, 0.8 & \text{Water,} \\ 1, 0, 10^5, 0.2 & \text{Air.} \end{cases} \qquad (18)$$

The stiffened gas equation of state parameters are $\gamma = 1.4$, $\pi = 0\,\mathrm{Pa}$ for air and $\gamma = 4.4$, $\pi = 6\times10^6\ \mathrm{Pa}$ for water.

The water-faucet test is used to assess developed numerical algorithms as it has an analytical solution. The analytical solution could be

derived by neglecting the pressure variation in liquid and interfacial drag between phases and assuming that the two components are incompressible. The analytical solutions for the water velocity and the evolution of the air volume fraction can be written as follows:

$$u_2(x,t) = \begin{cases} \sqrt{(u_2^0)^2 + 2g\,x} & \text{if } x \le u_2^0 t + \frac{1}{2} g t^2, \\ u_2^0 + gt & \text{otherwise,} \end{cases} \tag{19}$$

$$\alpha_1(x,t) = \begin{cases} 1 - \dfrac{\alpha_2^0 u_2^0}{\sqrt{(u_2^0)^2 + 2g\,x}} & \text{if } x \le u_2^0 t + \frac{1}{2} g t^2, \\ \alpha_1^0 & \text{otherwise.} \end{cases} \tag{20}$$

Simulations of this test are conducted using the CFL = 0.6 and the results are obtained at t = 0.4 s. Various mesh resolutions have been used to show the convergence of the numerical solution. The results of the air volume fraction and water velocity are shown in Figure 5. One can observe that increasing the resolution more than 1500 cells would not improve much the results as an overshot starts to grow as shown in Figure 5 (a). The same observation can be seen in the results of Saurel and Abgrall 1999a.

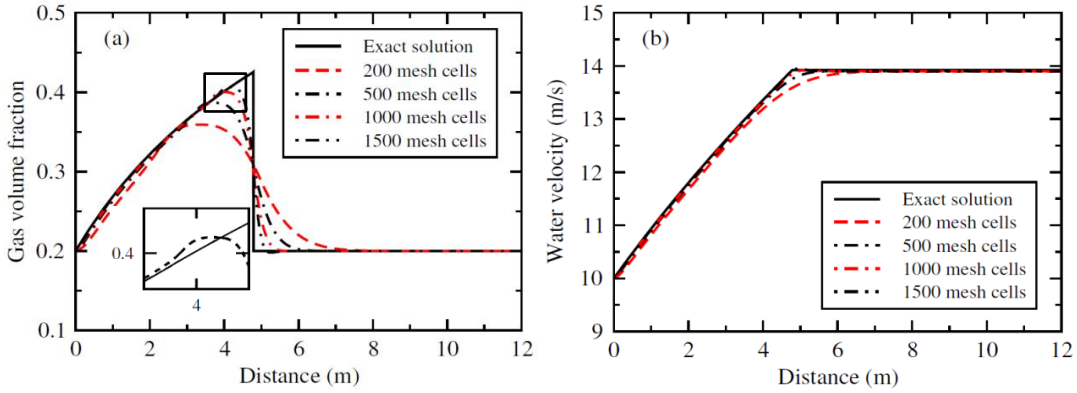

Figure 5. Water-faucet test: results using different mesh resolutions at t = 0.4 s for (a) air volume fraction and (b) water velocity.

5. Conclusions:

In this paper, the implementation of the DIM for two-phase flow based on an extended second order finite volume Godunov-type approach is done successfully. The assessment of the performance of the developed algorithm has been verified for high and low pressure regimes using benchmark test problems. Obtained results are in good agreement with the exact solution for water-air test and water-faucet test. However, overshot appears in the results of water-faucet test when very high number of cells is used.

6. References:

[1] Chanson, H. (1997). Air Bubble Entrainment in Free-Surface Turbulent Shear Flows. Academic Press, London, UK, (ISBN 0-12-168110-6).

[2] Mishima, K. and Hibiki, T. (1996) Some Characteristics of Air-water Two-phase Flow in Small Diameter Vertical Tubes. International Journal of Multiphase Flow, Volume 22, Issue 4, 703-712.

[3] Jolgam, S. A., Ballil, A. R., Nowakowski, A. F. and Nicolleau, F. C. G. A. (2012). Simulations of Compressible Multiphase Flows Through a Tube of Varying Cross-section. Proc. The ASME 2012 11th Biennial Conference on Engineering Systems Design and Analysis, Nantes, France.

[4] Shakibaeinia, A. (2015). Mesh-free Particle Modelling of Air-water Interaction. Proc. The 36th IAHR World Congress, Hague, Netherlands.

[5]Cocchi, J. P. and Saurel, R. (1997). A Riemann Problem Based Method for Compressible Multifluid Flows. Journal of Computational Physics. Volume 137, 265-298.

[6]Farhat, C. and Roux, F. X. (1991). A Method for Finite element Tearing and Interconnecting and its Parallel Solution Algorithm. International Journal of Numerical Methods in Engineering. Volume 32, Issue 6, 1205-1227.

[7]Hirt, C. W. and Nichols, B. D. (1981). Volume Of Fluid (VOF) method for the dynamics of free boundaries. Journal of Computational Physics. Volume 39, 201-255.

[8]Youngs, D. L. (1982). Time Dependent Multi-material Flow with Large Fluid Distortion (ed. K. W. Morton and M. J. Baines).Academic.

[9]Fedkiw, R. P., Aslam, T., Merriman, B. and Osher, S. (1999). A non Oscillatory Eulerian Approach to Interfaces in Multimaterial Flows (The Ghost Fluid Method). Journal of Computational Physics. Volume 152, 457-492.

[10] Karni, S. (1996) Hybrid Multifluid Algorithms. SIAM Journal of Scientific Computing. Volume 17, Issue 5, 1019-1039.

[11] Shyue, K. M. (1998). An Efficient Shock-capturing Algorithm for Compressible Multicomponent Problems, Journal of Computational Physics. Volume 142, 208-242.

[12]Saurel, R. and Abgrall, R. (1999). A Multiphase Godunov Method for Compressible Multifluid and Multiphase Flows. Journal of Computational Physics. Volume 150, 425-467.